

Collisional excitation of Na-Rydberg atoms

K. Batra^{1,a}, V. Prasad^{2,b}, and M. Mohan^{1,c}

¹ Department of Physics and Astrophysics, University of Delhi, Delhi-110007, India

² Swami Shradhanand College, University of Delhi, Delhi-110036, India

Received 26 December 2001 / Received in final form 8 April 2002

Published online 19 July 2002 – © EDP Sciences, Società Italiana di Fisica, Springer-Verlag 2002

Abstract. The scattering of heavy ion with a multilevel Rydberg atom in the presence of an electromagnetic field is studied. The interaction of Rydberg atom and the e.m field is explored using non-perturbative quasi-energy technique. Although the results are presented for selected excitations but in actual calculations we have included many levels of the atom. The effect of various parameters are shown on collisional excitation process. As an illustration detailed calculations are performed for the inelastic proton-Na Rydberg atom collision accompanied by the transfer of photons and the effects of dressing due to the field are considered. The emphasis of the present work is on collision induced transitions especially the case that involves change of orbital as well as principal quantum number.

PACS. 34.60.+z Scattering in highly excited states (e.g., Rydberg states)

1 Introduction

In the last few years, there has been a revival of interest in highly excited states due to the introduction of tunable lasers allowing for a selective preparation of Rydberg states [1–4]. Such a study has attracted considerable attention due to the unusual spectroscopic properties of Rydberg atoms. Due to its large size and dipole moment a Rydberg atom is one of the few systems that may be exposed to well controlled external fields. The classical prototypes for Rydberg states are alkali-metal atoms.

From the stand point of studying the basic physics of collision process we are particularly interested in approximate models which not only conserve the basic qualitative features, but also allow us to make substantial progress towards an analytic solution of the problem. With advances in experimental research on Rydberg atoms, excited states with very large quantum numbers ($n \simeq 600$) have been reported [5–7]. For such states the cross-sections for scattering of charged particles are extremely large. In order to describe transitions between such states, it is necessary to take an approach by which it is possible to find cross-sections for any arbitrary n . In the present paper we have developed a comprehensive formulation of collisional treatments suitable for Rydberg atom collisions with ions, based on the quasi-energy analysis of the time-dependent Schrödinger equation in the impact parameter approach.

The present study is devoted to collisionally aided radiative excitation of Na-Rydberg atom due to heavy ion

impact. This study is quite useful in the analysis of ion-atom collisions, for a quantitative modelling of low and high temperature plasmas [8–10]. These processes provide information on the interaction between colliding particles, on the trend of gas phase chemical reactions [11] and on ways to develop new types of lasers [12]. The study of collision induced population transfer has been reported earlier in a number of contexts. Seaton [13] calculated electron and proton impact excitation of $3s-3p$ transition in sodium for application to astrophysical processes. Bloomfield *et al.* [14,15] have observed resonant microwave multiphoton transitions between Rydberg states of potassium. Experimental results are also available on the total cross-sections for transitions from nd levels of the sodium atom [16]. It has been recognised that many properties of plasma are determined by the presence of atoms or ions in the excited states and lifetimes of these states are determined in part by collision with particles of the medium.

A knowledge of excitation cross-section is also important in many applications such as energy loss of heavy ions in solid targets, radiation damage in biological matters, plasma heating e.m waves etc. The relatively small electric fields present in such situations distort the highly excited Rydberg states. It is therefore of great interest to study the effect of small electric field on the collisional excitation of Na-Rydberg atom. The excitation of alkali Rydberg states from their ns ground states has been a popular subject, but the experimental study of alkali atom valence electron excitation has been scarce. In case of sodium we find impacts limited to H^+ , H_2^+ , H_3^+ , He^+ , Ne^+ . Theoretical treatment of the $p+Na(3s) \rightarrow p+Na(3p)$ processes has been

^a e-mail: kriti4oct@yahoo.co.in

^b e-mail: vnautiyal@himalaya.du.ac.in

^c e-mail: sneh@del12.vsnl.net.in

limited to Born approximation [17], close coupling [18], Vainshtein-Presnyakov-Sobelman [19] and also reported by Cavagnero [20]. Experiments involving H^+ , H_2^+ , He^+ and Ne^+ projectiles incident on the $Na(30s)$ and $Na(29d)$ have been reported by Rolfes *et al.* [21] with energies up to 4351 eV.

In the present work we have used the non-perturbative method developed by Agre and Rapport [22] to study the microwave field-sodium atom interactions and the effect of various collision and field parameters on the ion atom system undergoing collisions. We have studied here the collision of an incoming proton with a sodium atom initially in the state “ i ” (in the presence of single mode laser beam) moving to excited states “ j ”. The dynamics of the Rydberg electron driven by such a time-dependent field is complex, owing to the large number of energetically accessible states that are coupled by the field during the encounter and also due to the influence of two Coulombic potentials (projectile and the Rydberg core). The accurate computation of the energetically high lying Rydberg states requires a careful choice of the Rydberg wave functions, as they differ from their hydrogenic counterparts in their large spatial domains. The wavefunctions for the present problem have been computed with the help of radial wave functions of Picart *et al.* [23]. Excitations have been considered for a set of degenerate as well as non-degenerate states. In particular it turns out that the cross-sections in the energy range of interest here can be described adequately by considering a total of sixteen levels, amongst which the levels coupled with the microwave field form a type of ladder transitions because of the nearly same spacing amongst them. We have restricted ourselves to n lying between 40 to 43, however the generalization to other values of n can be done in a similar way. Because of the finite range of radiative coupling, we have used the concepts of single channel quantum defect theory (QDT) which assumes the constant values of quantum defects for s , p , d and f states. In the light of above discussion we have in the present paper calculated TDCS’s (total differential cross-sections) for Na-Rydberg atom with proton impact in the presence of microwave field. The present calculated results can be used for further experimental work.

The paper is organized as follows: in Section 2, we present a theoretical treatment of the inelastic scattering of protons by Rydberg atoms in the presence of microwave field and obtain results concerning the importance of the dressing of atomic states in the scattering process. Section 3 contains a discussion of our analytical results in the frame work of time dependent non-perturbative approach. Finally, Section 4 is devoted to concluding remarks about the process.

2 Theory

In this section we study the interaction between a Na-Rydberg atom and a collision partner in the presence of the microwave field. We assume that a specific Rydberg state of sodium has been prepared by some experimental arrangement. We consider a Rydberg state

of 40s Na atom. The most important part of the interaction is a potential “ V ” between the collision partner and the valence electron of the Rydberg atom. The valence electron of the Rydberg atom may be described by the wavefunction ψ_{nlm} where n , l , m define the principal, orbital and magnetic quantum numbers respectively.

The geometry of the problem is as follows: the target Rydberg atom is assumed to be stationary at the origin and the collisional partner, here proton, passes the target atom with an impact parameter “ b ” at $x = 0$ and is moving in the positive x -direction with a constant velocity \mathbf{v} . We assume that the projectile travels in a straight line and in addition there is an e.m field in the z -direction. This straight line trajectory provides a valid representation of the inelastic cross-sections.

We have assumed the dipole approximation to be valid here and have ignored small effects due to the recoil of the target and the projectile, as well as exchange effects and fine and hyperfine structures and all other interactions with the core. In accordance with Irby *et al.* [21] we isolate few levels from $n = 40$ to $n = 43$ states of Na atom from the entire set of energy levels. The e.m field is treated classically and is assumed to be purely monochromatic with angular frequency ω and linear polarization vector $\hat{\mathbf{e}}$. It is represented by:

$$\mathbf{E}(t) = \hat{\mathbf{e}}E_0 \cos(\omega t) \quad (1)$$

where E_0 is the amplitude of the e.m field. Using the atomic units we can write the time-dependent Schrödinger equation for the above ion-atom system in the presence of e.m field as:

$$i \frac{\partial \psi}{\partial t}(\mathbf{r}, t) = [H_0(\mathbf{r}) + V_{\text{int}}^L(\mathbf{E}, \omega, t) + V_{\text{int}}] \psi(\mathbf{r}, t) \quad (2)$$

where H_0 is the Hamiltonian of the atom in the absence of field and is given by:

$$H_0(\mathbf{r}) = T_{\text{kin}} + V_0. \quad (3)$$

The given operator H_0 determines the structure of the atom. The energy operator H_0 satisfies the equation:

$$H_0(\mathbf{r})u_q(\mathbf{r}) = E_q^0 u_q(\mathbf{r}) \quad (4)$$

where $u_q(\mathbf{r})$ are the unperturbed eigenfunctions corresponding to energies E_q^0 . The operator of the energy of the interaction of atom with the e.m field is given by:

$$V_{\text{int}}^L(\mathbf{E}, \omega, t) = -\mathbf{d} \cdot \mathbf{E} \quad (5)$$

where \mathbf{d} is the dipole moment operator and V_{int} describes the interaction potential between the projectile ion and the Rydberg atom. The interaction potential has been truncated to its dominant dipole term. The collisional excitation of Rydberg atoms has been extensively studied by others using this type of potential (*e.g.* in case of without field calculation Irby *et al.*). As far as charge dipole interaction is concerned, this potential reproduces the results of normalized Born approximations for fast collisions

and describes reasonably the slow collisions between levels with small quantum defects [5]. At far away distances (impact parameters) $V_{\text{int}} \rightarrow 0$, equation (2) reduces to the Schrödinger equation of isolated atom in the presence of e.m field *i.e.*

$$i \frac{\partial \phi}{\partial t}(\mathbf{r}, t) = H_A(\mathbf{r}, t)\phi(\mathbf{r}, t) \quad (6)$$

where

$$H_A(\mathbf{r}, t) = H_0(\mathbf{r}) + V_{\text{int}}^L(\mathbf{E}, \omega, t) \quad (7)$$

is the atomic Hamiltonian in the presence of e.m field. At low and intermediate values of the impact parameter there is an energy transfer to the Rydberg electron leading to a shake up process. The energy transfer is accounted by the differences in the proton plus the photon energies and the ionic core transition interval. There is however another aspect of present process that unlike the electron impact collisions, there is no exchange interaction between target and projectile to complicate the picture and the projectile transfers a small fraction of its momentum and energy during the collision.

In terms of quasi-energy formalism we express the quantum levels of the atom in terms of the dressed states. The dressed states provide a useful representation of the collision dynamics over a wide range of impact parameters and ion velocities and can be used conveniently with the Rydberg atoms because of their large polarizability. We expand the total wavefunction of the system in terms of the dressed states and bare states as:

$$\psi(\mathbf{r}, t) = \sum_n C_n \phi_n + \sum_m C_m \chi_m e^{-iE_m t} \quad (8)$$

where the subscript n runs over all the dressed states and m over all the bare states. The laser field couples only the angular momentum channels with $\Delta l = \pm 1$, so we have presently considered the $s \rightarrow p$ transitions for n ranging from 40 to 43 to be laser coupled due to the nearly same energy level spacing between them and their being dipole allowed. Substituting equation (8) into equation (2) and using the orthogonality condition we obtain a set of coupled first order differential equations

$$i \sum_n \frac{dC_n}{dt} = \sum_n C_n(t) \langle \phi_j | V | \phi_n \rangle + \sum_m C_m(t) \langle \phi_j | V | \chi_m \rangle e^{-iE_m t}. \quad (9)$$

The interaction potential between the incident proton and the atom is of the form

$$V = -\frac{Z}{R} + \sum_{j=1}^Z \frac{1}{r_{0j}} \quad (10)$$

where Z is the effective charge of the Rydberg atom, \mathbf{R} is the position coordinate of the incident proton and r_j is

the position vector of the j th atomic electron with respect to the atomic nucleus and

$$\frac{1}{r_{0j}} = \frac{1}{|R - r_j|}. \quad (11)$$

Under the assumption that radiation is nearly resonant and intensity being not too high we express the solution of the Schrödinger equation in terms of the dressed states as:

$$\phi_n(\mathbf{r}, t) = e^{-i(E_{40s} + \lambda_n)t} \sum_{m=1}^8 a_m^n u_m(\mathbf{r}) e^{-i(m-1)\omega t} \quad (12)$$

where the summation extends over all the bare states. In the present calculation we have considered the following eight states *i.e.* $40s \rightarrow 40p \rightarrow 41s \rightarrow 41p \rightarrow 42s \rightarrow 42p \rightarrow 43s \rightarrow 43p$. Here $u_m(\mathbf{r})$ are the unperturbed atomic states, E_{40s} is the energy of the 40s level, a_m^n are the amplitudes corresponding to the bare atomic states and λ_n are the quasi-energies. The summation can be generalized to any number of bare states (for multiplets).

For the present problem we cannot treat the bare wavefunctions as hydrogenic because of very large principal quantum numbers associated with the Rydberg atom. The Rydberg atom wavefunction is given in terms of radial and angular elements as

$$u_j(r) = R_{nl}(r) Y_{lm}(\theta', \phi') \quad (13)$$

where r , θ' and ϕ' define position of the Rydberg electron. The accurate computation of the wavefunction requires a careful choice of the radial part, therefore it is of vital importance to determine the correct value of the radial element. The use of coulomb approximation is hindered by the fact that the customary method of evaluation of radial integrals – that of Bates and Damgaard [24] breaks down due to the cancellation of large terms in the series when ν or ν' are large where ν , ν' define the effective principal quantum number for the initial and final states respectively. The method of Edmonds and Kelly [28] can deal with higher ν , ν' , but since it evaluates the integrals by numerical quadrature it becomes inefficient and eventually fails for large values. The present problem therefore requires a very special treatment so we are using an empirical approximation of Naccache [25] and Richards [26]. Naccache and Richards have applied the Heisenberg's correspondence principle to give the approximation to evaluate the square of the radial matrix elements between states $nl \rightarrow n'l'$ where n , n' are the principal quantum numbers and l , l' are the orbital quantum numbers for the initial and the final states respectively. It is given by:

$$|\langle nl|r|n'l' \rangle|^2 \simeq \left(\frac{n_c^2}{2s} \right)^2 [(1 + \Delta l l_c / n_c) J_{s+1}(s\epsilon) - (1 - \Delta l l_c / n_c) J_{s-1}(s\epsilon)] \quad (14)$$

where $\Delta l = l' - l$, $s = n - n'$, $l_c = \max(l, l')$, $n_c = 2/[1/n + 1/n']$ and ϵ is the eccentricity of the classical Kepler orbit. For purpose of extrapolation Picart *et al.* [23] considered

the ratio

$$\phi(nl, n'l') = \langle nl|r|n'l' \rangle / \left(\frac{3}{2} n_c^2 (1 - (l_c/n_c)^2)^{1/2} \right) \quad (15)$$

where the denominator is a good approximation to the non-hydrogenic matrix element $\langle n_c l | r | n_c l' \rangle$. Considering the maclaurin series for ϕ in terms of $\gamma = \Delta l l_c / n_c$

$$\phi(nl, n'l') = \sum_{p=0}^{\infty} \gamma^p f_p(s). \quad (16)$$

The coefficients of γ^p are functions of s and are given by Oertel and Shomo [27]. The series of ϕ truncated up to γ^3 , gives a good approximation to ϕ . This leads to a similar expression for the non-hydrogenic case given by:

$$\phi(\nu l, \nu' l') = \langle \nu l | r | \nu' l' \rangle / \left(\frac{3}{2} \nu_c^2 (1 - (l_c/\nu_c)^2)^{1/2} \right) \quad (17)$$

where $l_c = \max(l, l')$ and $\nu_c = 2/[1/\nu + 1/\nu']$. ν and ν' are the effective principal quantum number for the initial and the final states respectively. The difference $\nu - \nu' = s$ is not necessarily an integer and the series for nonhydrogenic case can be written as

$$\phi(\nu l, \nu' l') = \sum_{p=0}^{\infty} \gamma^p g_p(s). \quad (18)$$

The coefficients $g_p(s)$ are defined for all real s and share the symmetric properties of $f_p(s)$ above. The tabulation of the functions $g_0(s), g_1(s), g_2(s), g_3(s)$ for $|s| < 4.0$ has been done by Edmonds *et al.* [28]. We have restricted our study here to a small range of n *i.e.* $40 \leq n \leq 43$ because of the limitations on the value of s [28]. Considering the series summation up to γ^3 we arrive at:

$$\langle \nu l | r | \nu' l' \rangle = \left(\frac{3}{2} \nu_c^2 (1 - (l_c/\nu_c)^2)^{1/2} \right) \sum_{p=0}^3 \gamma^p g_p(s) \quad (19)$$

where $l_c, \nu_c, \Delta l, \nu, \nu', s$ are same as defined earlier and $\gamma = \Delta l (l_c/\nu_c)$.

We have calculated the radial matrix elements rigorously for all the sixteen levels considered including both dipole allowed and dipole forbidden transitions. These radial integrals have been used to determine the bare state wavefunctions for the Rydberg states which are then used to formulate the dressed state wavefunctions for the field coupled states. The set of coupled differential equations given by equation (9) have been solved by the non-perturbative quasi-energy technique using the dressed state formalism. In matrix form we can write the coupled differential equations as:

$$i\dot{C}(t) = Q(t)C(t) \quad (20)$$

where $C(t)$ is a column matrix and $Q(t)$ is a coupling matrix.

The above equations can be solved numerically for the time-dependent coefficients $c_j(t)$ for a particular set of initial conditions. Using the standard diagonalization technique as used by others [29, 30]. The coupled equation (20) can be solved at $t = +\infty$, we define

$$C(+\infty) = U \exp(-M_D) U^+ C(-\infty) \quad (21)$$

where U is a unitary operator and M_D is a diagonalized matrix obtained by the unitary transformation

$$M_D = U^+ M U \quad (22)$$

where

$$M = \int_{-\infty}^{+\infty} Q(t') dt'. \quad (23)$$

Using equation (21) we arrive at the transition probability for the transition for the state $i \rightarrow f$ given by

$$P_{i \rightarrow f} = |C_f(+\infty)|^2. \quad (24)$$

This probability can be integrated with respect to the impact parameter to find out the total cross-section for the transition from the initial state i to final state f as

$$\sigma_{i \rightarrow f} = 2\pi \int_0^{\infty} P_{i \rightarrow f}(b) b db. \quad (25)$$

In the next section we discuss the results thus obtained.

3 Discussion

A full quantum mechanical treatment of collisions aided excitations in Rydberg atoms in the presence of e.m field at any velocities is a highly impractical numerical integration problem so we have used impact parameter approximation to simplify the problem. A quantity which is very sensitive to the quality of calculated Rydberg orbitals is the so called quantum defect μ_l which depends on the orbital angular momentum l of the Rydberg electron. This quantum defect accounts for effective potential arising from the $(Z - 1)$ core electrons and a nucleus of charge Z by shifting the energy eigen-values away from the hydrogenic values. Since the scattering of charged particles with atoms is induced predominantly by the long range dipole interaction, then, within the velocity range considered here, the ion can be considered to move along classical trajectories. It has been assumed that the proton acts as a mere spectator at far away distances and this point is quite apparent from the graph of probability *vs.* impact parameter, where the graphs depict reduction in probability at large impact parameters (see Figs. 2 and 3).

The present study has been limited to a small range of n because of the limitation on the values of s , since the radial integrals considered and the truncated series representation of ϕ is valid only for $|\gamma| < 0.2$ and $|s| < 4.0$. Since the Rydberg atom has a very large radius and the electron probability distribution is peaked at very large

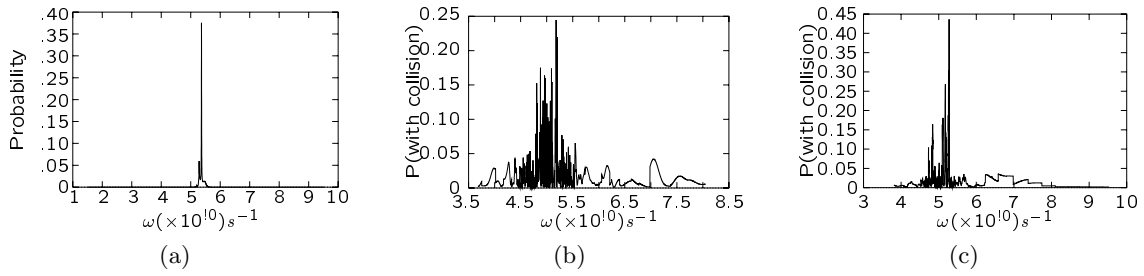


Fig. 1. (a) Probability for transition from $40s$ to $41p$ state in the absence of collision as a function of field frequency, at an intensity $I = 10$ mW/cm². (b) Probability for transition from $40s$ to $41p$ state in the presence of collision as a function of field frequency, at an intensity $I = 100$ mW/cm². (c) Probability for transition from $40s$ to $41p$ state in the presence of collision as a function of field frequency, at an intensity $I = 10$ mW/cm².

distances from the parent ion thereby leading to very low kinetic energies of the Rydberg electron, therefore the velocities of the incident projectiles have been taken larger than the velocity of the Rydberg electron. Charge transfer mechanism is not included in the theoretical model considered here because of large collision velocities.

For finding out the collisional probabilities, first of all, the dressed states have been calculated. Once the dressed states are known, one can solve the coupled differential equations by the diagonalization technique, for the transition amplitudes $c_j(t)$ with the initial condition $c_i = 1$, $c_j(j \neq i) = 0$. Usually the initial condition is $c_i = \delta_{oi}$ which implies the atom being in the ground state at $t = 0$, but here it implies the atom to be in the $40s$ state, which may happen due to some other process such as excitation by pulsed laser or collisional excitation. Substituting $C(+\infty)$ in equation (24) one gets the transition probabilities. Finally the cross-sections $\sigma_{i \rightarrow j}$ are evaluated by integrating the transition probability $P_{i \rightarrow j}$ with respect to the impact parameter. The results are also shown in the light of without field calculations.

In Figure 1 we present the variation of transition probabilities with the field frequency. Figure 1a shows the variation of probability for $40s$ – $41p$ transition with frequency, at an intensity $I = 10$ mW/cm² in the absence of collision. The transition probability rises sharply at $\omega = 5.36 \times 10^{10}$ s⁻¹ (0.0814 eV), corresponding to the three photon resonance. The same transition has been studied for collisional impact with the proton and the maxima is observed at $\omega = 5.18 \times 10^{10}$ s⁻¹ with intensity $I = 100$ mW/cm² (see Fig. 1b) and at $\omega = 5.28 \times 10^{10}$ s⁻¹ with intensity $I = 10$ mW/cm² (see Fig. 1c) showing how the transition probability is modified by the collision process. The maxima observed for collisional impact fall in a range of frequencies near the resonance frequency.

The variation of probability without collision as a function of field frequency is also shown for $40s$ – $40p$ transition with maxima satisfying one photon resonance ($\omega = 5.506 \times 10^{10}$ s⁻¹) (Fig. 4).

Figures 2 and 3 is a plot between probability and impact parameter b , at incident particle velocity $v = 0.04$ a.u., and field frequency $\omega = 5.506 \times 10^{10}$ s⁻¹. Figure 2 is drawn for the $40s$ – $40p$ transition at a field in-

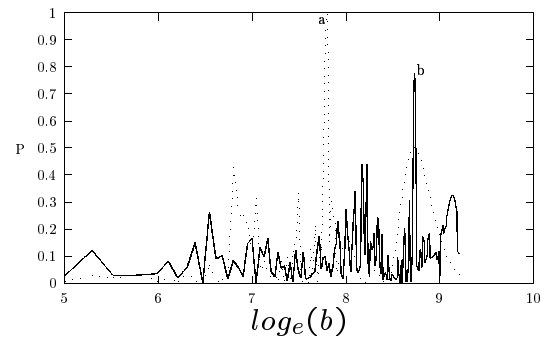


Fig. 2. The probability for transition from $40s$ to $40p$ state as a function of impact parameter ($\log_e(b)$) at collision velocity $v = 0.04$ a.u. (a) in the absence of field, and (b) in the presence of field with intensity $I = 1$ W/cm² and frequency $\omega = 5.506 \times 10^{10}$ s⁻¹.

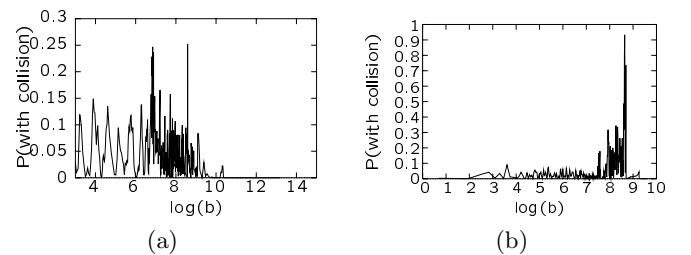


Fig. 3. (a) The probability for transition from $40s$ to $40d$ state as a function of impact parameter ($\log_e(b)$) at collision velocity $v = 0.04$ a.u., frequency $\omega = 5.506 \times 10^{10}$ s⁻¹ and intensity $I = 1$ W/cm². (b) The probability for transition from $40s$ to $40p$ state as a function of impact parameter ($\log_e(b)$) at collision velocity $v = 0.04$ a.u., frequency $\omega = 5.506 \times 10^{10}$ s⁻¹ and intensity $I = 10$ mW/cm².

tensity $I = 1$ W/cm². A comparison has been made for the without field case and the effect of field modifying the collision is shown. The same transition is also studied at a field intensity $I = 10$ mW/cm² (see Fig. 3b) and it is observed that for low intensities (Fig. 3b) the probability is larger ($P^L = 9.33 \times 10^{-1}$) than at higher intensity ($P^L = 7.9 \times 10^{-1}$) (Fig. 2) as expected.

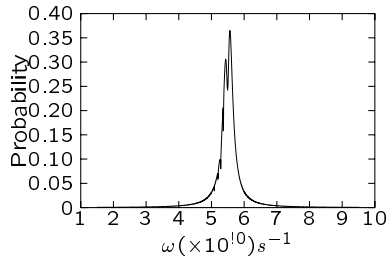


Fig. 4. The probability (without collision) for transition from $40s$ to $40p$ state as a function of field frequency ω , at an intensity $I = 10$ mW/cm².

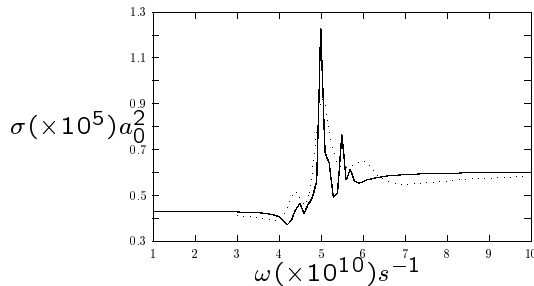


Fig. 5. Cross-section for transition from $40s$ to $40p$ state as a function of field frequency ω , with collision velocity $v = 0.04$ a.u. at an intensity $I_1 = 1$ mW/cm² (bold line) and $I_2 = 10$ mW/cm² (dotted line).

In general the transition probabilities oscillates at small values of b and decreases to zero at large b . This type of variation in transition probability is a general feature of the collision problem and can be explained on the basis of multichannel coupling effect. At large impact parameters, the interaction is weak and the transition probability is small. Also it is seen that the maximum transition probability $P^L(40s-40p)$ (7.9×10^{-1}) has a much greater magnitude than $P^L(40s-40d)$ (2.52×10^{-1}) (see Fig. 3a) at the same intensity, since the earlier satisfies one photon resonance at $\omega = 5.506 \times 10^{10}$ s⁻¹.

The cross-section for the collisional excitation of Na Rydberg atom has been measured as a function of incident particle velocity and field frequency. Figures 5 to 8 show a variation of cross-section with field frequency for the collision velocity $v = 0.04$ a.u. Figure 5 describes the variation in cross-section for the transition $40s \rightarrow 40p$ at an intensity $I = 1$ mW/cm². It shows a sharp rise in cross-section at $\omega = 5.00 \times 10^{10}$ s⁻¹ and a small rise at $\omega = 5.506 \times 10^{10}$ s⁻¹ explaining how the collision process modifies the transition with peaks shifted from resonance to near resonance. The same transition has been studied at a higher intensity $I = 10$ mW/cm². It is observed that the cross-section is maximum at near resonance frequency for both cases but there is a shake up process at high intensities that leads the probability to flow to other channels.

Figure 6 shows the variation of cross-section with field frequency for $40s \rightarrow 41p$ at an intensity $I = 1$ mW/cm². The peak is observed at $\omega = 5.2 \times 10^{10}$ s⁻¹, which is near to three photon resonance ($\omega = 5.356 \times 10^{10}$ s⁻¹). Figure 7

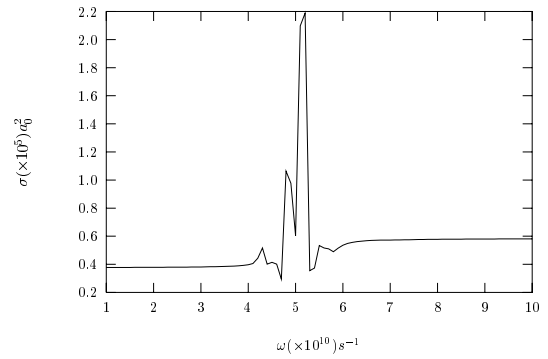


Fig. 6. Cross-section for transition from $40s$ to $41p$ state as a function of field frequency ω at an intensity $I = 1$ mW/cm² and collision velocity $v = 0.04$ a.u.

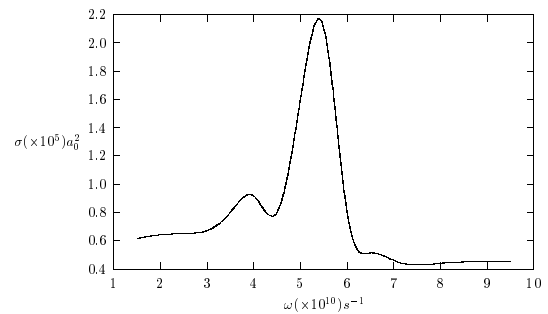


Fig. 7. Cross-section for transition from $40s$ to $43s$ state as a function of field frequency ω , at an intensity $I = 100$ mW/cm² and collision velocity $v = 0.04$ a.u.

shows the same variation for the transition $40s \rightarrow 43s$ at an intensity $I = 100$ mW/cm² with peak near to the six photon resonance frequency ($\omega = 5.096 \times 10^{10}$ s⁻¹).

We have studied these variations for the dipole forbidden transition also. Figures 8a and 8b show the variations in cross-sections for the $40s \rightarrow 40d$ transitions with field frequency at intensities $I = 1$ mW/cm² and $I = 10$ mW/cm² respectively. This particular transition is although not field coupled but the field frequency and intensity modifies the cross-section to a significant level. At higher intensities it is modified as earlier ($40s \rightarrow 40p$).

Figure 9 shows how cross-section varies with collision velocity for three different transitions at an intensity $I = 1$ mW/cm². Figure 9a shows the variation for $40s \rightarrow 40p$ at one photon resonance frequency ($\omega = 5.50 \times 10^{10}$ s⁻¹). It is seen that cross-section decreases both at low as well as at high velocities. The same variation is seen in Figure 9b for the transition $40s \rightarrow 40d$ drawn for eight photon resonance and Figure 9c for the transition $40s \rightarrow 40f$ drawn for nine photon resonance (both dipole forbidden). On comparison it is apparent that for velocities near the target electron the p -states become decoupled from the manifold leading to greater rise in cross-section for the dipole forbidden transitions. These results are in good accord with the results earlier obtained [31–34].

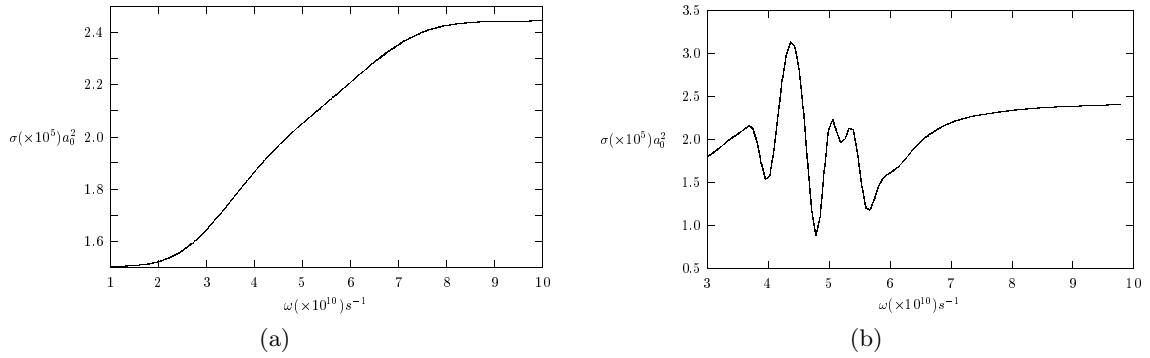


Fig. 8. (a) Cross-section for transition from $40s$ to $40d$ state as a function of field frequency ω , at an intensity $I = 1 \text{ mW/cm}^2$ and collision velocity $v = 0.04 \text{ a.u.}$ (b) Cross-section for transition from $40s$ to $40d$ state as a function of field frequency ω , at an intensity $I = 10 \text{ mW cm}^{-2}$ and collision velocity $v = 0.04 \text{ a.u.}$

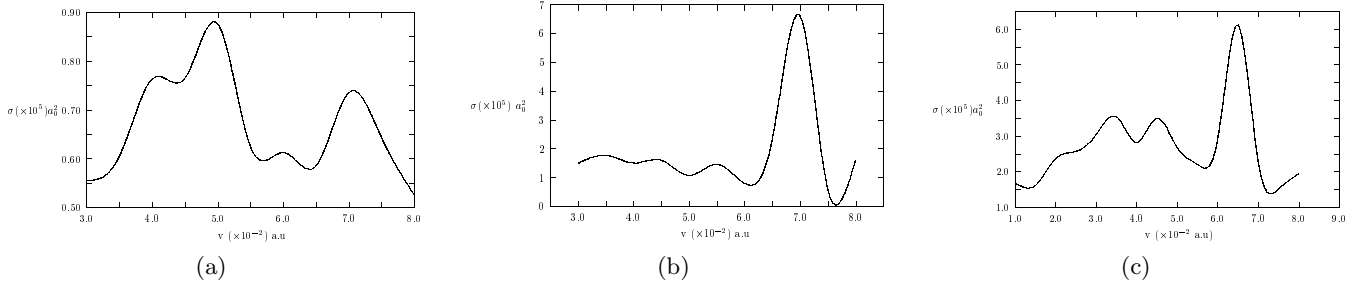


Fig. 9. (a, left) Cross-section for transition from $40s$ to $40p$ state as a function of collision velocity at an intensity $I = 1 \text{ mW/cm}^2$ and frequency $\omega = 5.506 \times 10^{10} \text{ s}^{-1}$ (one photon resonance). (b, center) Cross-section for transition from $40s$ to $40d$ state as a function of collision velocity at an intensity $I = 1 \text{ mW/cm}^2$ and frequency $\omega = 1.80 \times 10^{10} \text{ s}^{-1}$ (eight photon resonance). (c, right) Cross-section for transition from $40s$ to $40f$ state as a function collision velocity at an intensity $I = 1 \text{ mW/cm}^2$ and frequency $\omega = 1.62 \times 10^{10} \text{ s}^{-1}$ (nine photon resonance).

4 Summary and conclusion

The observed collision process is a very good example of ion-atom collision. As such it is of interest from a fundamental point of view because it is theoretically tractable and experimentally accessible. We have described a combination of the non-perturbative quasi-energy approach for the radiation-atom interaction and the close-coupling impact parameter method for the collision-aided radiative excitation of a dressed atom. The ion-Rydberg atom collision has been treated using the quantum defect theory. The use of quasi-energy non-perturbative approach has the potential of revealing the entire information about the collisional process. The collisional field excitation has been studied preferably because collisional field excitation is interesting from a basic physics perspective, as it adds complexity to the one electron field excitation process. The results obtained are consistent with the earlier models. The variations of cross-sections with collision velocity and field frequency describes the process very effectively.

KB acknowledges the help from Council of Scientific and Industrial Relations (CSIR) for financial support. MM is thankful to UGC and DST for financial support.

References

1. K.A. Safinya, J.F. Delpech, F. Gounand, W. Sandner, T.F. Gallger, *Phys. Rev. Lett.* **47**, 405 (1981)
2. T.F. Gallger, K.A. Safinya, F. Gounand, J.F. Delpech, W. Sandner, R.D. Kachru, *Phys. Rev. A* **25**, 1905 (1982)
3. D.S. Thompson, R.C. Stoneman, T.F. Gallger, *Phys. Rev. A* **39**, 2914 (1989)
4. T.F. Gallger, *Phys. Rep.* **210**, 319 (1992)
5. I.L. Beigman, M.I. Syrkin, *Sov. Phys. JETP* **62**, 226 (1985)
6. A.A. Konovalenko, L.G. Sodin, *Nature* **283**, 360 (1978); **294**, 135 (1981)
7. D.H. Blake, R.H. Crutcher, W.D. Watson, *Nature* **287**, 707 (1980)
8. M.H. Mittleman, *Introduction to the Theory of electron-Atom Collisions* (Plenum, New York, 1982)
9. *Photon Assisted Collisions and Related Topics*, edited by N.K. Rahman, C. Guidotti (Academic, New York, 1992)
10. M. Mohan, V. Prasad, *J. Phys. B* **24**, L81 (1991)
11. L.I. Gudzenko, L.V. Gurvich, V.S. Dubov, S.I. Yakovenko, *Sov. Phys. JETP* **46**, 1082 (1977)
12. T.F. George, *J. Phys. Chem.* **86**, 10 (1986)
13. M.J. Seaton, *Proc. Phys. Lond.* **79**, 1105 (1962)
14. L.A. Bloomfield, R.C. Stoneman, T.F. Gallger, *Phys. Rev. Lett.* **57**, 2512 (1986)
15. R.C. Stoneman, D.S. Thompson, T.F. Gallger, *Phys. Rev. A* **37**, 1527 (1988)

16. K. Mac Adam, R. Rolfes, D. Crosby, *Phys. Rev. A* **24**, 1286 (1981)
17. C. Kubach, V. Sidis, *Phys. Rev. A* **23**, 110 (1981)
18. R.J. Bell, B.G. Skinner, *Proc. Phys. Soc. Lond.* **80**, 404 (1962)
19. C.E. Theodosiou, *Phys. Rev. A* **36**, 2067 (1987)
20. M.J. Cavagnero, *Phys. Rev. A* **52**, 2865 (1995)
21. V.D. Irby, R.G. Rolfes, O.P. Makarov, K.B. Mac Adam, M.I. Syrkin, *Phys. Rev. A* **52**, 3809 (1995)
22. Ya.M. Agre, L.P. Rapport, *Sov. Phys. JETP* **55**, 215 (1982)
23. J. Picart, A.R. Edmonds, N. Tran Minh, *J. Phys. B* **11**, L651 (1978)
24. D.R. Bates, A. Damgaard, *Phil. Trans. R. Soc.* **242**, 101 (1949)
25. P.F. Naccache, *J. Phys. B: At. Mol. Phys.* **5**, 1308 (1972)
26. I. Percival, D. Richards, *Adv. At. Mol. Phys.* **11**, 1 (1975)
27. G.K. Oertel, L.P. Shomo, *Astrophys. J. Suppl.* **16**, 175 (1968)
28. A.R. Edmonds, J. Picart, N. Tran Minh, R. Pullen, *J. Phys. B* **12**, 2781 (1979)
29. B. Sharma, M. Mohan, *J. Phys. B* **19**, L433 (1986)
30. J. Callaway, E. Baur, *Phys. Rev. A* **140**, 1072 (1965)
31. M.I. Syrkin, *Phys. Rev. A* **53**, 825 (1996)
32. R.G. Rolfes, L.G. Gray, O.P. Makarov, K.B. Mac Adam, *J. Phys. B* **26**, 2191 (1993)
33. R.G. Rolfes, L.G. Gray, K.B. Mac Adam, *J. Phys. B* **25**, 2319 (1992)
34. R.G. Rolfes, V.D. Irby, O.P. Makarov, R.C. Dickinson, K.B. Mac Adam, *J. Phys. B* **27**, 1167 (1994)